

Influence of air exposure duration and a-Si capping layer thickness on the performance of p-BaSi₂/n-Si heterojunction solar cells

| | |
|------------------------------|--|
| 著者別名 | 都甲 薫, 末益 崇 |
| journal or publication title | AIP Advances |
| volume | 6 |
| number | 8 |
| page range | 085107 |
| year | 2016-08 |
| 権利 | (C) 2016 Author(s). All article content, except where otherwise noted, is licensed under a Creative Commons Attribution (CC BY) license (http://creativecommons.org/licenses/by/4.0/). |
| URL | http://hdl.handle.net/2241/00144247 |

doi: 10.1063/1.4961063



Influence of air exposure duration and a-Si capping layer thickness on the performance of p-BaSi₂/n-Si heterojunction solar cells

Ryota Takabe, Suguru Yachi, Weijie Du, Daichi Tsukahara, Hiroki Takeuchi, Kaoru Toko, and Takashi Suemasu

Citation: *AIP Advances* **6**, 085107 (2016); doi: 10.1063/1.4961063

View online: <http://dx.doi.org/10.1063/1.4961063>

View Table of Contents: <http://scitation.aip.org/content/aip/journal/adva/6/8?ver=pdfcov>

Published by the [AIP Publishing](#)

Articles you may be interested in

[Effect of amorphous Si capping layer on the hole transport properties of BaSi₂ and improved conversion efficiency approaching 10% in p-BaSi₂/n-Si solar cells](#)

Appl. Phys. Lett. **109**, 072103 (2016); 10.1063/1.4961309

[p-BaSi₂/n-Si heterojunction solar cells with conversion efficiency reaching 9.0%](#)

Appl. Phys. Lett. **108**, 152101 (2016); 10.1063/1.4945725

[Theoretical simulations of the effects of the indium content, thickness, and defect density of the i-layer on the performance of p-i-n InGaN single homojunction solar cells](#)

J. Appl. Phys. **108**, 093118 (2010); 10.1063/1.3484040

[Spectroscopic aspects of front transparent conductive films for a-Si thin film solar cells](#)

J. Appl. Phys. **107**, 034505 (2010); 10.1063/1.3298932

[Effects of a-Si:H layer thicknesses on the performance of a-Si:H/c-Si heterojunction solar cells](#)

J. Appl. Phys. **101**, 054516 (2007); 10.1063/1.2559975

The advertisement features a blue and orange background with a molecular structure graphic. On the left is a thumbnail of an 'Applied Physics Reviews' journal cover. The main text reads 'NEW Special Topic Sections' in large white font. Below this, it says 'NOW ONLINE' in orange, followed by 'Lithium Niobate Properties and Applications: Reviews of Emerging Trends' in white. The AIP Applied Physics Reviews logo is in the bottom right corner.

NEW Special Topic Sections

NOW ONLINE
Lithium Niobate Properties and Applications:
Reviews of Emerging Trends

AIP Applied Physics Reviews

Influence of air exposure duration and a-Si capping layer thickness on the performance of p-BaSi₂/n-Si heterojunction solar cells

Ryota Takabe,¹ Suguru Yachi,¹ Weijie Du,² Daichi Tsukahara,¹
 Hiroki Takeuchi,¹ Kaoru Toko,¹ and Takashi Suemasu^{1,a}

¹*Institute of Applied Physics, University of Tsukuba, Tsukuba, Ibaraki 305-8573, Japan*

²*Key Laboratory of Optoelectronic Material and Device, College of Mathematics and Science, Shanghai Normal University, Shanghai 200234, China*

(Received 2 May 2016; accepted 2 August 2016; published online 10 August 2016)

Fabrication of p-BaSi₂(20nm)/n-Si heterojunction solar cells was performed with different a-Si capping layer thicknesses ($d_{\text{a-Si}}$) and varying air exposure durations (t_{air}) prior to the formation of a 70-nm-thick indium-tin-oxide electrode. The conversion efficiencies (η) reached approximately 4.7% regardless of t_{air} (varying from 12–150 h) for solar cells with $d_{\text{a-Si}} = 5$ nm. In contrast, η increased from 5.3 to 6.6% with increasing t_{air} for those with $d_{\text{a-Si}} = 2$ nm, in contrast to our prediction. For this sample, the reverse saturation current density (J_0) and diode ideality factor decreased with t_{air} , resulting in the enhancement of η . The effects of the variation of $d_{\text{a-Si}}$ (0.7, 2, 3, and 5 nm) upon the solar cell performance were examined while keeping $t_{\text{air}} = 150$ h. The η reached a maximum of 9.0% when $d_{\text{a-Si}}$ was 3 nm, wherein the open-circuit voltage and fill factor also reached a maximum. The series resistance, shunt resistance, and J_0 exhibited a tendency to decrease as $d_{\text{a-Si}}$ increased. These results demonstrate that a moderate oxidation of BaSi₂ is a very effective means to enhance the η of BaSi₂ solar cells. © 2016 Author(s). All article content, except where otherwise noted, is licensed under a Creative Commons Attribution (CC BY) license (<http://creativecommons.org/licenses/by/4.0/>). [<http://dx.doi.org/10.1063/1.4961063>]

I. INTRODUCTION

For future deployment of terawatt-scale solar cells, extensive research has been conducted on thin-film solar cell materials such as chalcopyrite and cadmium telluride as well as Si-based materials because of their high energy conversion efficiency (η) and low cost.^{1–6} Perovskite-based solar cells have also gained increasing attention owing to their astonishing increase in efficiency.^{7,8} However, these materials contain critical raw materials such as In, Cd, and Pb. There has also been growing interest in Si thin-film solar cells that employ an efficient light-trapping system,^{9–15} but with this system it is not easy to achieve an η as high as 20%. Hence, it is necessary to explore alternative materials for thin-film solar cell applications. Among such materials, much attention has been given to the semiconductor BaSi₂, which consists of safe and earth-abundant elements and has a band gap (E_g) of 1.3 eV, matching the solar spectrum.¹⁶ One of the most striking features of this material is that both its large absorption coefficient (α) and large minority-carrier diffusion length (L) can be used. Because of its indirect band gap, undoped BaSi₂ can attain a minority-carrier lifetime (τ) and an L value as large as approximately 10 μs and 10 μm , respectively.^{17–19} These values are sufficiently large for thin-film solar cell applications. Furthermore, α exceeds $3 \times 10^4 \text{ cm}^{-1}$ for photon energies greater than 1.5 eV because the direct transition occurs at energies slightly larger than E_g .^{20–22} For these reasons, we expect η to be larger than 25% in a 2- μm -thick BaSi₂ pn junction diode.²³

^asuemasu@bk.tsukuba.ac.jp



An a-Si capping layer plays an important role in BaSi₂ solar cells, whereby an undoped n-BaSi₂ surface with a few nm-thick a-Si layer can exhibit a $\tau = \sim 10$ μs with excellent repeatability.²⁴ Measurements of the valence band offset at the a-Si/BaSi₂ interface by hard x-ray photoelectron spectroscopy have shown that the barrier height of the a-Si layer for the minority carrier (i.e., holes) in the n-BaSi₂ is -0.2 eV,²⁵ whereas that of the native oxide layer is 3.9 eV.²⁶ Therefore, the a-Si capping layer works as a good electrical contact for hole transport as well as a passivation layer. Very recently, we have attained $\eta = 9.0\%$, a short-circuit current density $J_{\text{SC}} = 31.9$ mA/cm² and an open-circuit voltage $V_{\text{OC}} = 0.46$ V for B-doped p-BaSi₂/n-Si heterojunction solar cells using an a-Si capping layer.²⁷ The a-Si layer thickness ($d_{\text{a-Si}}$) and the duration of air exposure (t_{air}) after a-Si layer deposition are important parameters that may influence the performance of BaSi₂ solar cells. Previous studies have shown that t_{air} and $d_{\text{a-Si}}$ have a significant effect upon the performance of a-Si:H(n)/a-Si:H(i)/c-Si(p) heterojunctions with intrinsic thin layer (HIT) solar cells.²⁸ This sensitivity arises from the significant influence the t_{air} and i-layer thickness have upon the minority-carrier transport and recombination at the interfaces in HIT solar cells.²⁸ However, there is limited information regarding their effects upon BaSi₂ solar cells. In this work, we fabricated a-Si/p-BaSi₂(20 nm)/n-Si heterojunction solar cells via molecular beam epitaxy (MBE) prepared with various values of t_{air} and $d_{\text{a-Si}}$, and attempted to clarify the influence of these parameters upon the properties of p-BaSi₂/n-Si solar cells.

II. EXPERIMENTS

For the growth of the BaSi₂ layers, we used an ion-pumped MBE system (AVC Co., Ltd.) equipped with an electron-beam evaporation source for Si and with standard Knudsen cells for Ba and B. The deposition rates of Si (R_{Si}) and Ba (R_{Ba}) were controlled using an electron impact emission spectroscopy (EIES) feedback system (INFICON CO., Ltd). We first deposited Ba on a heated Czochralski n-Si(111) (resistivity $\rho = 1\text{--}4$ $\Omega\text{-cm}$) substrate at 500°C by reactive deposition epitaxy to form a 5-nm-thick BaSi₂ template layer,²⁹ where R_{Ba} was set at 1.0 nm/min. This template layer acted as seed crystals for the subsequent BaSi₂ layer. We next co-deposited Ba, Si and B on the templates at 600°C by MBE to form a 20-nm-thick B-doped p-BaSi₂ layer,^{30–32} where R_{Si} and R_{Ba} were fixed at 0.9 and 2.3 nm/min, respectively. The B concentration was set to 2×10^{18} cm⁻³ to be comparable to the hole concentration.²⁷ The epitaxial growth of the BaSi₂ layers in all of the samples was confirmed by reflection high-energy electron diffraction and x-ray diffraction (data not shown). We first prepared four samples (samples A–D) to examine the influence of t_{air} upon the solar cell performance. For this purpose, we deposited a 2 or 5-nm-thick a-Si layer on the BaSi₂ surface *in situ* at 180°C with $R_{\text{Si}} = 0.9$ nm/min, followed by air exposure for $t_{\text{air}} = 12$ or 150 h. In the previous study,²⁵ we found that the oxidation of BaSi₂ do not progress for sample capped with 5-nm-thick a-Si layers even for $t_{\text{air}} = 24$ h. Therefore, we anticipated that the oxidation of BaSi₂ would be suppressed much further for $t_{\text{air}} = 12$ h. On the other hand, we expected that the oxidation would progress for $t_{\text{air}} = 150$ h. This is the reason why we chose these two air exposure durations. As described below, the η increased with t_{air} for samples with $d_{\text{a-Si}} = 2$ nm. We next prepared samples in which $d_{\text{a-Si}}$ was varied from 0.7 to 5 nm while keeping $t_{\text{air}} = 150$ h to examine the influence of $d_{\text{a-Si}}$. Please note that the a-Si layers in this study were not hydrogenated. They were just evaporated from the solid source of Si by electron beam irradiation. After keeping samples in air for t_{air} , each sample was introduced into a radio-frequency (RF) sputtering chamber, and 1-mm-diameter and 70-nm-thick indium-tin-oxide (ITO) electrodes were sputtered on the front and Al electrodes on back surfaces at room temperature. The RF power was set to 100 W. The solar cell properties of samples A–D are summarized in Table I.

The plots of the current density versus voltage (J - V) were measured for as many electrodes as possible in an area of 1×1 cm² on the sample wafer under AM1.5, 100 mW/cm² illumination at approximately 25°C using a mask with holes 1 mm in diameter. To accurately obtain the series resistance, R_{S} , diode ideality factor, γ , and reverse saturation current density, J_0 , of a diode, we adopted a technique described in Ref. 33. Using the photodiode equation, the relationship between

TABLE I. Sample and solar cell parameters for samples A–D, giving the thickness of the a-Si layer ($d_{\text{a-Si}}$), duration of exposure to air (t_{air}), short-circuit current density (J_{SC}), open-circuit voltage (V_{OC}), fill factor (FF), conversion efficiency (η), series resistance (R_{S}), shunt resistance (R_{SH}), diode ideality factor (γ) and reverse saturation current density (J_0).

| Sample | $d_{\text{a-Si}}$ (nm) | t_{air} (h) | J_{SC} (mA/cm ²) | V_{OC} (V) | FF | η (%) | R_{S} (Ω) | R_{SH} (k Ω) | γ | J_0 (mA/cm ²) |
|--------|---------------------------|-------------------------|--|------------------------|------|---------------|--------------------------------|----------------------------------|----------|--------------------------------|
| A | 2 | 12 | 30.5 | 0.34 | 0.51 | 5.3 | 178 | 36.1 | 1.58 | 1.02×10^{-2} |
| B | 2 | 150 | 29.5 | 0.44 | 0.51 | 6.6 | 336 | 20.4 | 1.29 | 2.35×10^{-4} |
| C | 5 | 12 | 22.5 | 0.42 | 0.50 | 4.8 | 125 | 12.3 | 1.26 | 4.14×10^{-5} |
| D | 5 | 150 | 28.1 | 0.40 | 0.42 | 4.7 | 322 | 11.8 | 1.44 | 8.73×10^{-4} |

R_{S} and γ can be given as

$$\frac{dV}{dJ} = SR_{\text{S}} + \frac{\gamma k_{\text{B}} T}{q} \left[\frac{1 - (SR_{\text{SH}})^{-1} dV/dJ}{J + J_{\text{SC}} - (SR_{\text{SH}})^{-1} V} \right]. \quad (1)$$

Here, T is the absolute temperature, q is the elemental charge, k_{B} is the Boltzmann constant, S is the area of the electrode, R_{SH} is the shunt resistance, and J_{SC} is the photocurrent density. Using the plot of dV/dJ versus the term in brackets in Eq. (1), we can directly deduce γ from the slope and R_{S} from the intercept. The external quantum efficiency (EQE) spectra were evaluated at 25°C using a lock-in technique with a xenon lamp and a 25-cm focal-length single monochromator (Bunko Keiki, SM-1700A).

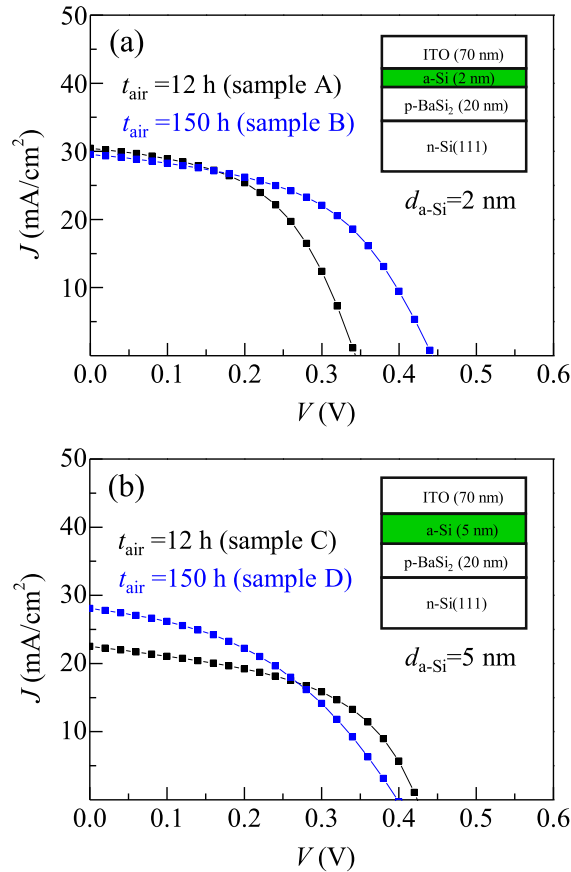


FIG. 1. J - V characteristics under AM1.5 illumination measured for samples with $d_{\text{a-Si}}$ = (a) 2 nm (samples A and B) and (b) 5 nm (samples C and D). The t_{air} was varied as 12 or 150 h.

III. RESULTS AND DISCUSSION

First we discuss the influence of t_{air} on the solar cell performance. Figure 1(a) and 1(b) show typical examples of the J - V characteristics under AM1.5 illumination on samples with $d_{\text{a-Si}} = 2$ nm (samples A and B, Fig. 1(a)) and 5 nm (samples C and D, Fig. 1(b)), for t_{air} of 12 or 150 h. As shown in Fig. 1(a), V_{OC} drastically increases with increasing t_{air} for samples with $d_{\text{a-Si}} = 2$ nm, and η was improved from 5.3 to 6.6%, as shown in Table I. Meanwhile, V_{OC} decreases with increasing t_{air} for samples with $d_{\text{a-Si}} = 5$ nm, while J_{SC} increases and η remains approximately constant at 4.7%. As shown in Table I, R_{S} increases with t_{air} regardless of $d_{\text{a-Si}}$, meaning that part of the a-Si and/or BaSi₂ layer became oxidized during the exposure of the samples to air. In our previous study, we found that τ was improved when the oxygen composition in the region close to the BaSi₂ surface became large.²² We thus speculate that the oxygen concentration became higher in the BaSi₂ region close to the a-Si/BaSi₂ interface for samples with $d_{\text{a-Si}} = 2$ nm than for those with $d_{\text{a-Si}} = 5$ nm when t_{air} was increased. This increase in oxygen concentration may lead to a reduction of the surface recombination and thereby a decrease in J_0 . It was indeed found that J_0 decreased by approximately 1/50 in sample B ($d_{\text{a-Si}} = 2$ nm) compared with sample A ($d_{\text{a-Si}} = 2$ nm) after 150 h, as shown in Table I. In an ideal case, V_{OC} is given by

$$V_{\text{OC}} \approx \frac{k_{\text{B}}T}{q} \exp\left(\frac{J_{\text{SC}}}{J_0}\right). \quad (2)$$

It is therefore reasonable that V_{OC} becomes larger by increasing t_{air} . Meanwhile, J_{SC} increased but the fill factor (FF) and V_{OC} decreased with increasing t_{air} for samples at $d_{\text{a-Si}} = 5$ nm because J_0 increased by more than 20 times and R_{S} increased. The increase of J_{SC} likely arises from the decrease of absorption in the a-Si layer owing to its partial oxidation, as will be discussed later. Although the mechanism behind the large increase of J_0 at $t_{\text{air}} = 150$ h is not clear at present, it is safe to state that η is improved with increasing t_{air} when the a-Si layer thickness is small.

We next discuss the influence of $d_{\text{a-Si}}$ upon the solar cell performance when $t_{\text{air}} = 150$ h. Figure 2 shows typical examples of the J - V characteristics under AM1.5 illumination where $d_{\text{a-Si}}$ varies as 0.7, 2, 3, and 5 nm. It can be seen that the J - V curves significantly depend upon $d_{\text{a-Si}}$ and, in particular, the sample with $d_{\text{a-Si}} = 0.7$ nm exhibits J - V characteristics similar to those obtained without an a-Si capping layer (results in Ref. 27). To understand this result, we compared the solar cell properties of p-BaSi₂/n-Si heterojunction solar cells fabricated with varying $d_{\text{a-Si}}$, as shown in Fig. 3. Some variation can be expected in the solar cell parameters, but it can be seen in Fig. 3 that there is a definite dependence of the solar cell parameters upon $d_{\text{a-Si}}$. When the a-Si layer was thinnest (0.7 nm), the R_{S} value was relatively large. This large R_{S} value suggests that it is possible to oxidize BaSi₂ with a sufficiently thin a-Si layer,²⁵ which could also explain the similar J - V curves

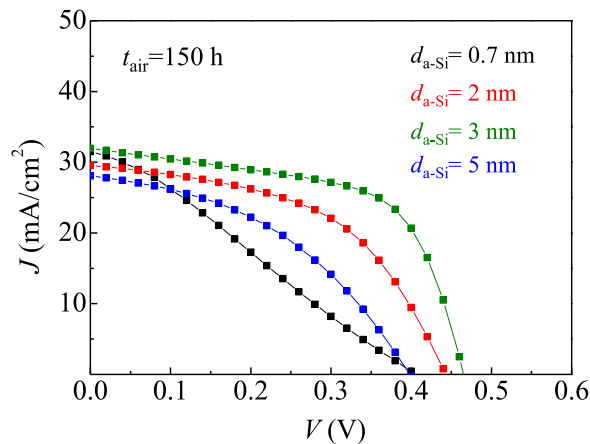


FIG. 2. J - V characteristics under AM1.5 illumination measured for samples whose $d_{\text{a-Si}}$ varies as 0.7, 2, 3, or 5 nm. The t_{air} was fixed at 150 h.

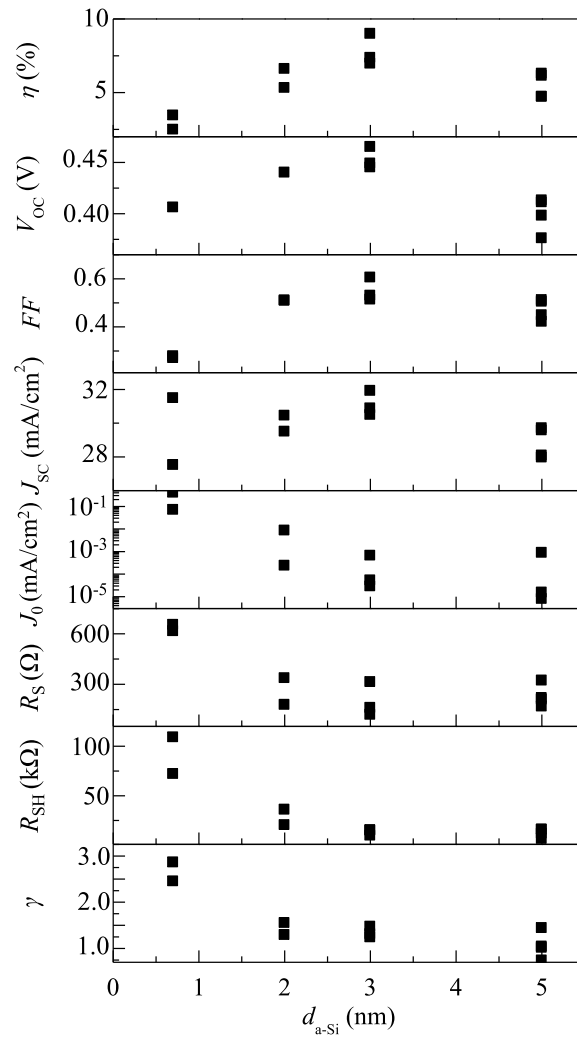


FIG. 3. Solar cell parameters of the p-BaSi₂/n-Si heterojunction solar cells, plotted as a function of d_{a-Si} . The t_{air} was fixed at 150 h.

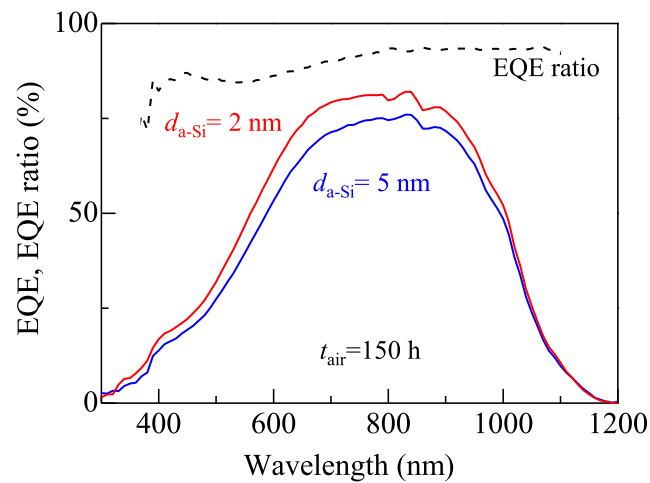


FIG. 4. EQE spectra for samples with $d_{a-Si} = 2$ and 5 nm. The t_{air} was fixed at 150 h. The broken line shows the ratio of EQE at $d_{a-Si} = 5$ nm to that at $d_{a-Si} = 2$ nm.

for samples with $d_{\text{a-Si}} = 0.7$ nm and those without a-Si capping layers. In addition, the η value reached a maximum of 9.0% when $d_{\text{a-Si}}$ was 3 nm and exhibited a decrease at $d_{\text{a-Si}} = 5$ nm, which was a trend echoed by the V_{OC} value. This is likely caused by a reduction of J_{SC} for $d_{\text{a-Si}} = 5$ nm because other parameters such as J_0 , R_{S} , R_{SH} and γ were seen to decrease with increasing $d_{\text{a-Si}}$, and to almost saturate at $d_{\text{a-Si}} = 3$ nm. To clarify this reason, we compared the external quantum efficiency (EQE) spectra for the samples with varying $d_{\text{a-Si}}$.

Figure 4 shows the EQE spectra for typical samples with $d_{\text{a-Si}} = 2$ and 5 nm, where the broken line shows the ratio of EQE at $d_{\text{a-Si}} = 5$ nm to that at $d_{\text{a-Si}} = 2$ nm. The EQE spectra are seen to decrease as $d_{\text{a-Si}}$ increases, especially in the wavelength range shorter than ~ 730 nm, which is equivalent to the bandgap energy of a-Si (1.7 eV). Therefore, it is reasonable to conclude that the reduction in J_{SC} arises from the light absorption within the a-Si layer. This result is similar to that reported in HIT solar cells,²⁸ and we thus attribute the reduction of J_{SC} to the same optical loss caused by the absorption in the a-Si layer. Therefore, a further increase in $d_{\text{a-Si}}$ may be found to reduce η .

IV. CONCLUSION

We fabricated a-Si/B-doped p-BaSi₂(20 nm)/n-Si heterojunction solar cells with various t_{air} and $d_{\text{a-Si}}$ values, and investigated the influence of these varying parameters upon the solar cell performance. Solar cell parameters such as η , V_{OC} , J_{SC} , J_0 , R_{S} , γ , and R_{SH} were found to depend upon t_{air} and $d_{\text{a-Si}}$. The η value increased from 5.3 to 6.6% as t_{air} increased from 12 to 150 h for samples with $d_{\text{a-Si}} = 2$ nm. When t_{air} was fixed at 150 h, the η value reached a maximum of 9.0% at $d_{\text{a-Si}} = 3$ nm. These results reveal that the precise control of BaSi₂ oxidation can enhance η much further.

ACKNOWLEDGEMENTS

This work was supported in part by the Core Research for Evolutional Science and Technology (CREST) project of the Japan Science and Technology Agency (JST) and by a Grant-in-Aid for Scientific Research A (No. 15H02237) from the Japan Society for the Promotion of Science (JSPS). R.T. was financially supported by a Grant-in-Aid for JSPS Fellows (No. 15J02139).

- ¹ I. Repins, M. A. Contreras, B. Egaas, C. DeHart, J. Scharf, C. L. Perkins, B. To, and R. Noufi, *Prog. Photovoltaics* **16**, 235 (2008).
- ² H. Katagiri, K. Jimbo, W. S. Maw, K. Oishi, M. Yamazaki, H. Araki, and A. Takeuchi, *Thin Solid Films* **517**, 2455 (2009).
- ³ S. Niki, M. Contreras, I. Repins, M. Powalla, K. Kushiya, S. Ishizuka, and K. Matsubara, *Prog. Photovolt: Res. Appl.* **18**, 453 (2010).
- ⁴ C. Li, Y. Wu, J. Poplawsky, T. J. Pennycook, N. Paudel, W. Yin, S. J. Haigh, M. P. Oxley, A. R. Lupini, M. Al-Jassim, S. J. Pennycook, and Y. Yan, *Phys. Rev. Lett.* **112**, 156103 (2014).
- ⁵ P. Jackson, D. Hariskos, R. Wuerz, O. Kiowski, A. Bauer, T. M. Friedlmeier, and M. Powalla, *Phys. Stat. Solidi RRL* **9**, 28 (2015).
- ⁶ S. Merdes, F. Ziem, T. Lavrenko, T. Walter, I. Laueremann, M. Klingsporn, S. Schmidt, F. Hergert, and R. Schlattmann, *Prog. Photovoltaics* **23**, 1493 (2015).
- ⁷ J. Burschka, N. Pellet, Soo-Jin Moon, R. Humphry-Baker, P. Gao, M. K. Nazeeruddin, and Michael Grätzel, *Nature* **499**, 316 (2013).
- ⁸ N. J. Jeon, J. H. Noh, W. S. Yang, Y. C. Kim, S. Ryu, J. Seo, and S. I. Seok, *Nature* **517**, 476 (2015).
- ⁹ H. Sasaki, H. Morikawa, Y. Matsuno, M. Deguchi, T. Ishihara, H. Kumabe, T. Murotani, and S. Mitsui, *Jpn. J. Appl. Phys. Part 1* **33**, 3389 (1994).
- ¹⁰ J. Müller, B. Rech, J. Springer, and M. Vanecek, *Sol. Energy* **77**, 917 (2004).
- ¹¹ A. V. Shah, H. Schade, M. Vanecek, J. Meier, E. Vallat-Sauvain, N. Wyrsch, U. Kroll, C. Droz, and J. Bailat, *Prog. Photovolt: Res. Appl.* **12**, 113 (2004).
- ¹² J. Haschke, D. Amkreutz, L. Korte, F. Ruske, and B. Rech, *Sol. Energy Mater. Sol. Cells* **128**, 190 (2014).
- ¹³ A. Bozzola, P. Kowalczewski, and L. C. Andreani, *J. Appl. Phys.* **115**, 094501 (2014).
- ¹⁴ O. Isabella, J. Krc, and M. Zeman, *Appl. Phys. Lett.* **97**, 101106 (2010).
- ¹⁵ H. Sai, Y. Kanamori, and M. Kondo, *Appl. Phys. Lett.* **98**, 113502 (2011).
- ¹⁶ K. Morita, Y. Inomata, and T. Suemasu, *Thin Solid Films* **508**, 363 (2006).
- ¹⁷ M. Baba, K. Toh, K. Toko, N. Saito, N. Yoshizawa, K. Jiptner, T. Sakiguchi, K. O. Hara, N. Usami, and T. Suemasu, *J. Cryst. Growth* **348**, 75 (2012).
- ¹⁸ K. O. Hara, N. Usami, K. Toh, M. Baba, K. Toko, and T. Suemasu, *J. Appl. Phys.* **112**, 083108 (2012).
- ¹⁹ K. O. Hara, N. Usami, K. Nakamura, R. Takabe, M. Baba, K. Toko, and T. Suemasu, *Appl. Phys. Express* **6**, 112302 (2013).

- ²⁰ D. B. Migas, V. L. Shaposhnikov, and V. E. Borisenko, *Phys. Status Solidi B* **244**, 2611 (2007).
- ²¹ K. Toh, T. Saito, and T. Suemasu, *Jpn. J. Appl. Phys.* **50**, 068001 (2011).
- ²² M. Kumar, N. Umezawa, and M. Imai, *J. Appl. Phys.* **115**, 203718 (2014).
- ²³ T. Suemasu, *Jpn. J. Appl. Phys.* **54**, 07JA01 (2015).
- ²⁴ R. Takabe, K. O. Hara, M. Baba, W. Du, N. Shimada, K. Toko, N. Usami, and T. Suemasu, *J. Appl. Phys.* **115**, 193510 (2014).
- ²⁵ R. Takabe, H. Takeuchi, W. Du, K. Ito, K. Toko, S. Ueda, A. Kimura, and T. Suemasu, *J. Appl. Phys.* **119**, 165304 (2016).
- ²⁶ R. Takabe, W. Du, K. Ito, H. Takeuchi, K. Toko, S. Ueda, A. Kimura, and T. Suemasu, *J. Appl. Phys.* **119**, 025306 (2016).
- ²⁷ D. Tsukahara, S. Yachi, H. Takeuchi, R. Takabe, W. Du, M. Baba, Y. Li, K. Toko, N. Usami, and T. Suemasu, *Appl. Phys. Phys.* **108**, 152101 (2016).
- ²⁸ H. Fujiwara and M. Kondo, *J. Appl. Phys.* **101**, 054516 (2007).
- ²⁹ Y. Inomata, T. Nakamura, T. Suemasu, and F. Hasegawa, *Jpn. J. Appl. Phys.* **43**, 4155 (2004).
- ³⁰ Y. Inomata, T. Nakamura, T. Suemasu, and F. Hasegawa, *Jpn. J. Appl. Phys.* **43**, L178 (2004).
- ³¹ R. Takabe, K. Nakamura, M. Baba, W. Du, M. A. Khan, K. Toko, M. Sasase, K. O. Hara, N. Usami, and T. Suemasu, *Jpn. J. Appl. Phys.* **53**, 04ER04 (2014).
- ³² M. Ajmal Khan, K. O. Hara, W. Du, M. Baba, K. Nakamura, M. Suzuno, K. Toko, N. Usami, and T. Suemasu, *Appl. Phys. Lett.* **102**, 112107 (2013).
- ³³ J. R. Sites and P. H. Mauk, *Solar Cells* **27**, 411 (1989).